Simple Models for Predicting the Post-fracture Behaviour of Laminated Glass

In the Proceedings of the XXV A.T.I.V 2010 International Conference, Parma, Italy. November 2010

Shelton NHAMOINESU and Mauro OVEREND Dept of Engineering
University of Cambridge,UK, sn393@cam.ac.uk, mo318@cam.ac.uk

1.0 ABSTRACT

The post-fracture strength of laminated glass is difficult to predict without resorting to costly prototype testing due to poorly described post-fracture phenomena that hinder the creation of simple analytical and numerical design models. This paper describes our recent efforts to create and experimentally validate numerical and simple analytical models of close-to-reality crack geometries of two-ply annealed glass with polyvinyl butyral (PVB) interlayer subjected to through-crack tension (TCT), offset-crack tension (OCT) and four-point bending (4PB) tests. The results of this research indicate that the models presented may be used for predicting the post-fracture behaviour of laminated glass and with improvements the models can be useful in large-scale commercial applications.

2.0 INTRODUCTION

The through-crack tension test TCT test was previously defined and used by Muralidhar *et al.* [1] to develop a bridging force-displacement relationship in terms of bulk polymer constitutive properties and interfacial toughness. Prior to that, Sha *et al.* [2] also used similar tests to estimate the interfacial fracture toughness between glass and PVB. Iwasaki *et al.* [3] used TCT to calculate the fracture toughness of glass-PVB laminates at various strain rates.

Our research builds on the work mentioned above by extending the TCT models to other close-to-reality geometries. In Section 3.0 we start by describing the TCT tests carried out on specimens with different interlayer thicknesses. We then describe OCT and 4PB tests before comparing the different force-extension curves from all the tests. In Section 4.0 we first review a simple analytical model of the TCT based on the peel test model of flexible laminates put forward by Kinlock *et al.* [4]. We then extend this model to the four-point bending test. Section 5.0 is dedicated to the description of experiments done to determine time-dependant visco-elastic and time-independent elasto-plastic properties of the PVB interlayer which were required for numerical modelling but could not be found in existing literature. Numerical modelling of the TCT is then presented in Section 6.0. Finally, the experimental validation of the models, conclusions and highlights of future work are all presented in Section 7.0

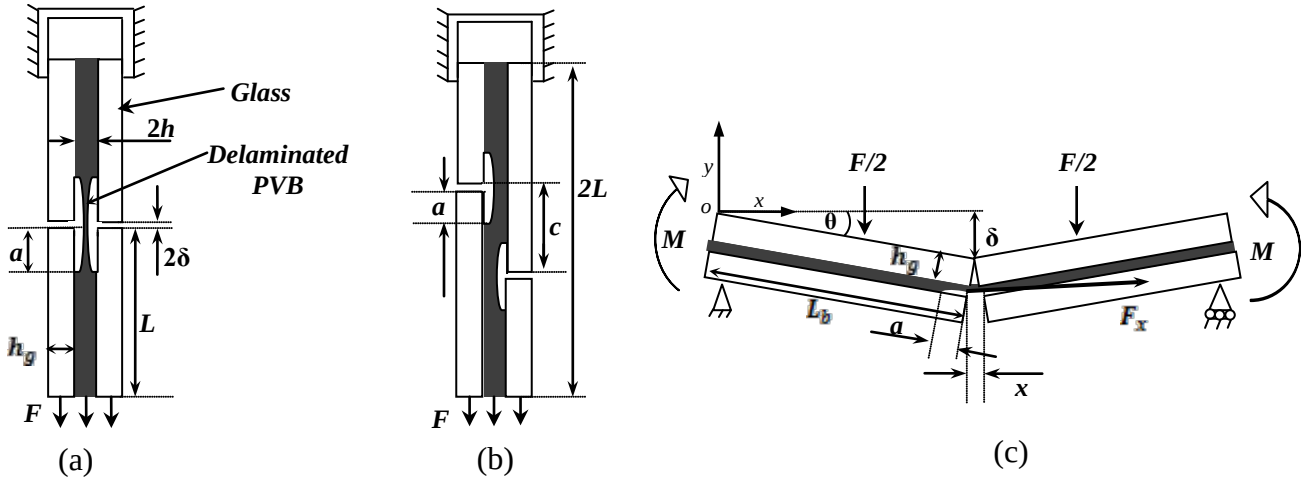

Figure 1: Schematic drawings of (a) The TCT test. (b) The OCT test. (c) The four-point bending test.

3.0 EXPERIMENTAL PROCEDURES AND RESULTS

The TCT and OCT specimens tested have length *2L=150mm* and width *b=50mm*. They are made of *6+2h+6 mm* laminated annealed glass with a PVB interlayer with thickness *2h*. Different samples with *2h = 0.38mm, 0.76mm and 1.52mm* have been prepared for the TCT test by scoring and pre-cracking the glass at length *L=75mm*. The tests have been carried out on an Instron 5500R electro mechanical test machine at displacement rates of *0.264mm/s* and *0.0264mm/s*. The applied tension force *F* is recorded with respect to the displacement *2δ*. The final delamination length *a* is also measured.

Figures 2(a) shows the plots of force versus extension δ at fast and slow displacement rates. Generally, all plots show an initially constant and high stiffness which can be attributed to the initiation of delamination as well as an initially small unbonded interlayer length. A yield point is then reached where it appears that a steady-state force has been reached. This observation suggests that in this steady-state force region, *a/δ* is constant as reported by Muralidhar *et al.* [1]. The subsequent drop in force observed in the graphs coincides with the tearing of the interlayer.

The offset crack tension OCT shown in fig 1(b) represents a more realistic failure mechanism of laminated glass as real-life cracks on two plies of a laminate are unlikely to be co-planar. Tensile tests, similar to those described for the TCT above, are carried out on the OCT specimens; the stiffness and the failure load are an order of magnitude higher than the TCT but the plastic deformation is considerably lower than the TCT due to the shear resistance in the overlap region C. As the shear progress - almost linearly - failure of one of the glass plies occurs and its position coincides with the pre-crack of the other glass ply, effectively turning the OCT into a TCT configuration.

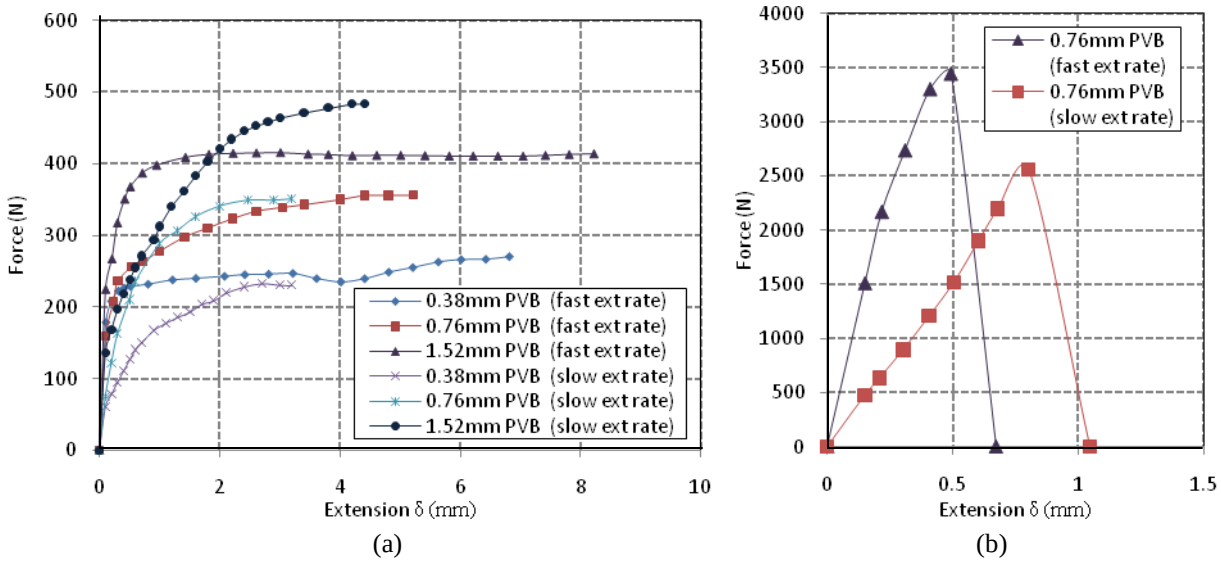

Figure 2: Force-Extension plots for (a) the TCT tests (b) the OCT tests

Figure 1(c) shows the four point bending tests performed on laminates of length $2L_b$*=350mm* and width *b=150mm*. The results of the four-point bending tests are compared to the TCT by converting force-displacement plots of the TCT to bending moment-hinge rotation plots (Fig 3). The results show that the moments per unit metre of crack length for the TCT are twice as high as those for the four point bending. This could be caused by the fact that in the 4PB test, not all of the interlayer thickness participates in the extension and delamination due to the orientation of the force with respect to the interlayer.

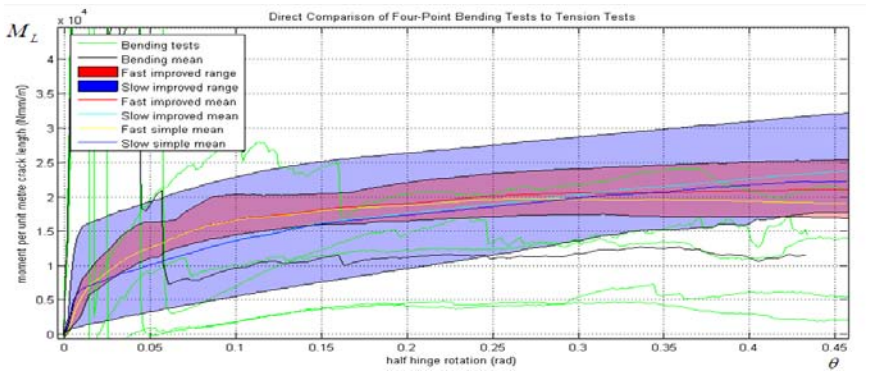

Figure 3: Direct comparison of tension results to four-point bending tests

4.0 ANALYTICAL MODEL: THE ENERGY BALANCE APPROACH

A practical approach for investigating delamination behaviour is the direct extraction of fracture energy from experiments. In this section, we therefore review and modify an analytical formulation for the extraction of fracture energy G_a from the TCT test. Kinloch *et al.* [4] and Muralidhar *et al.* [1] have shown that the adhesive fracture energy G_a may be derived from an energy-balance argument whereby the external work dU_{ext} done by the applied force F is balanced by (i) the stored strain energy in the interlayer dU_s, (ii) the energy dissipated during tensile deformation of the interlayer dU_{dt} and (iii) the work required to increase the fracture length a by an incremental extension da such that:

$$G_a = \frac{1}{b}\left(\frac{dU_{ext}}{da} - \frac{dU_s}{da} - \frac{dU_{dt}}{da}\right), \qquad (1)$$

Consider, from the schematic drawing of the TCT test shown in fig 1(a) above, an interlayer of thickness h and width b which is peeling in a steady state under a constant load F fig 1(a), then:

$$dU_{ext} = F da \varepsilon_a , \qquad (2)$$

and

$$d(U_s + U_{dt}) = bhda \int_0^{\varepsilon_a} \sigma \, d\varepsilon \qquad (3)$$

where ε_a is the steady state strain in the interlayer and $\int_0^{\varepsilon_a} \sigma \, d\varepsilon$ defines the elastic strain energy density $U(\varepsilon_L)$. Using (2) and (3) to expand equation (1) we obtain:

$$G_a = \frac{1}{b}\left(\frac{F da \varepsilon_a}{da} - \frac{bhda}{da}\int_0^{\varepsilon_a} \sigma \, d\varepsilon\right) = \frac{F\varepsilon_a}{b} - h\int_0^{\varepsilon_a} \sigma \, d\varepsilon = h\left(\frac{F\varepsilon_a}{hb} - \int_0^{\varepsilon_a} \sigma \, d\varepsilon\right), \qquad (4)$$

Equation (4) can then be used to extract the fracture energy G_a from the TCT tests provided the constitutive model for the interlayer is known, since the applied force F and the steady state strain can be measured from the experiment.

The TCT model described above can be extended to describe the four-point bending test shown in fig 1(c) above. Taking moments about the origin o it can be shown that the tensile force in the interlayer F_x is a function of the applied bending force F and half the hinge angle θ where:

$$\sin\theta = \frac{\delta}{L_b} \qquad (5)$$

and δ is the vertical displacement of the hinge contact point and L_b is half the length of the pre-cracked specimen. Assuming equilibrium and taking moments about the origin o, we have:

$$\sum M_o = \left(\frac{L_b}{2}\right)\left(\frac{F}{2}\right)\cos\theta - F_x\delta = 0 \;\Rightarrow\; F_x = \left(\frac{L_b F}{4\delta}\right)\cos\theta = \frac{F}{4\tan\theta} \qquad (6)$$

The interlayer extension x can in turn be expressed in terms of the thickness of the glass h_g and the hinge angle as follows:

$$x = 2h_g \sin\theta \quad (7)$$

Under steady state conditions, the strain in the interlayer ε_a is defined as the proportional increase in x with increasing delamination length a such that $\varepsilon_a = x/a$ which substituted into equation 7 yields:

$$\varepsilon_a = \frac{2h_g \sin\theta}{a} = \frac{2h_g \delta}{aL_b} \quad (8)$$

The energy balance equation (4) used for the TCT can now be implemented for the four point bending case by substituting the steady state strain ε_a from equation (8). Therefore, the fracture energy G_a can be extracted from the four point bending test of pre-cracked laminates using equation (9) below:

$$G_a = \frac{Fh_g}{2baL_b \tan\theta} - h\int_0^{\varepsilon_a} \sigma \, d\varepsilon \quad (9)$$

5.0 EXPERIMENTAL DETERMINATION OF PVB MATERIAL PROPERTIES

Finite Element models of the TCT test on *LUSAS v14.3* require an accurate constitutive model of the PVB interlayer. Existing literature does not seem to have decomposed time-dependant visco-elastic and time-independent elasto-plastic properties of PVB therefore tests on dumbbells sized to comply with *BSI, 1996a* [5] have been undertaken. These tests provide (i) the visco-elastic shear modulus G_v (ii) the visco-elastic decay constant β and (iii) the elasto-plastic stress-strain plots of PVB. The dumbbells have been cut from 1.52mm thick PVB sheets before being cured in an autoclave for approximately 6 hours under a temperature cycle reaching 135^0C at a maximum pressure of 6 bar until specimens were clear.

The visco-elastic properties G_v and β have been determined by applying a high strain-rate to the dumbbells up to a predefined extension followed by a period of unchanged extension while the decay of the load was recorded. The stress-time relationship (fig 4a) is converted to shear modulus-time relationship (fig 4b) from which $\beta = 0.002$ is obtained by curve fitting and $G_v = 4.1MPa$ is calculated by subtracting the experimentally determined residual shear modulus G_∞ from the initial shear modulus G_0.

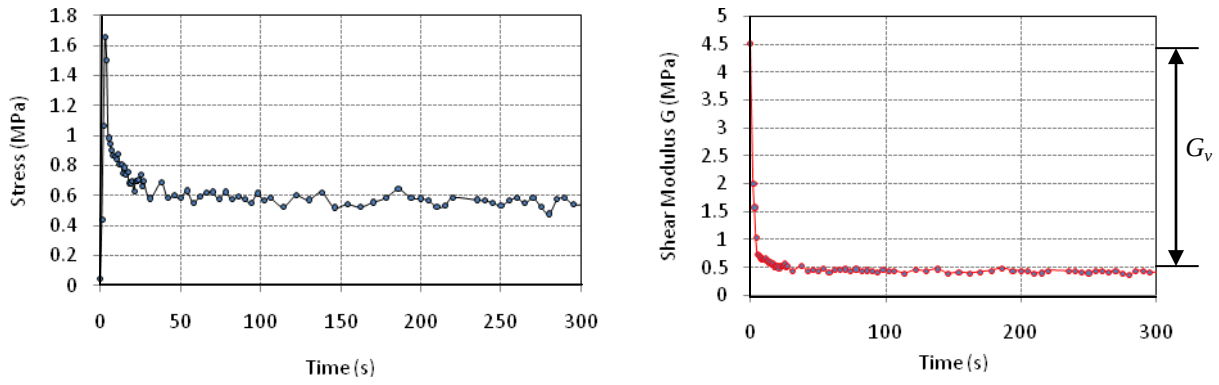

(a) (b)

Figure 4: (a) Stress vs. time curve of PVB dumbbell (b) Shear Modulus vs. time curve for PVB dumbbell

The elasto-plastic properties of the PVB have been determined by using a discrete load-step strategy on the dumbbell specimens. The total loading period is divided into approximately 30 intervals and at each interval; the load is increased by 5N and the specimen is allowed to relax for a period equal to the decay time t_d which is approximated at *180s* from Fig 4(a). A plot of these discrete increments followed by curve fitting of all discrete stable points gives a load-displacement

relationship that is independent of the viscous decay of the PVB (figure 5a). Therefore, the elasto-plastic stress-strain relationship (figure 5b) is obtained by curve fitting to the stable points.

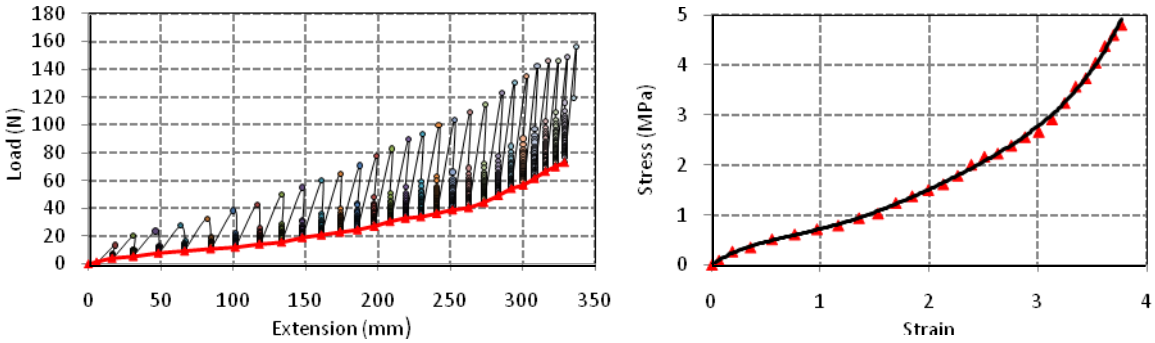

(a) (b)

Figure 5: (a) Load vs. Extension curve for elasto-plastic test on PVB dumbbell (b) Time-independent stress vs. strain relationship of PVB

6.0 NUMERICAL MODEL

The TCT test was constructed as a 2D FE model (figure 6) using LUSAS v14.3. Three node triangular plane strain elements (TPN3) were used. Due to symmetry, only a quarter of the TCT test was modelled as shown in figure 6 below. The glass was clamped by jaws from the top edge for a distance of 30mm shown by line DE. The model is symmetrical about line yy which is the mid-thickness of the 1.52mm PVB interlayer. The interface between PVB and glass was modelled using 2D interface elements (IPN6). The material properties of the interface elements are defined by (i) the fracture energy G_a and (ii) the initiation stress. The visco-elastic and elasto-plastic material properties of PVB obtained from experiments in section 5.0 were applied accordingly to the model. The glass is modelled as a perfectly linear elastic material with $E = 70GPa$ and $v = 0.23$. The solution experiences less convergence problems when a coarse mesh is used.

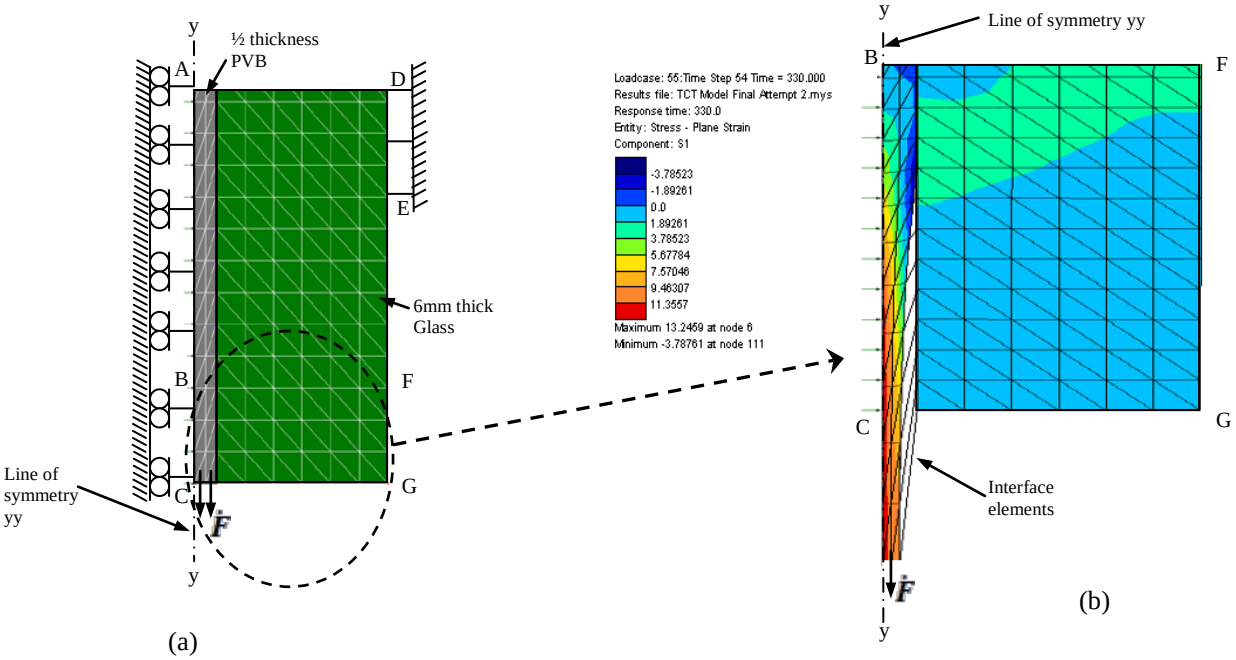

(a) (b)

Figure 6: FE model of TCT test (a) full model before extension (b) enlarged model area BCGF after velocity $\dot{F}$ has been applied

The velocity $\dot{F}$ applied to the lower boundary of the interlayer matches the displacement rate used in the TCT experimental tests. A nonlinear transient analysis is performed with an initial load case of one time step of 0.001 of the total time response followed by a second load case with a total duration similar to the experimental durations of the TCT test. An updated Langrangian approach was selected to capture geometric and material nonlinearity and prevent mesh penetration. [6, 7]

7.0 SUMMARY OF RESULTS AND FUTURE WORK

A comparison of delamination lengths a from the FE simulation with those from the TCT experiment at specific times show that the numerical simulation is in agreement with the TCT experiment when the fracture energy G_{α} applied on the model is approximately 940J/m^2 (fig 7a). The numerical model can therefore be used as a tool for directly estimating the fracture energy from a TCT test. A comparison of the experimental load versus extension curve with numerical simulations shows that the model reasonably predicts the extension behaviour of the TCT although it overestimates experimental results by a margin of almost 100N (fig 7b). Further work is required to develop experimental tests capable of separately extracting mode 1 (opening) and mode 2 (shear) fracture energies in order to improve the accuracy of the numerical models. Numerical models of pre-cracked laminates subjected to 4PB will also be developed based on the TCT models.

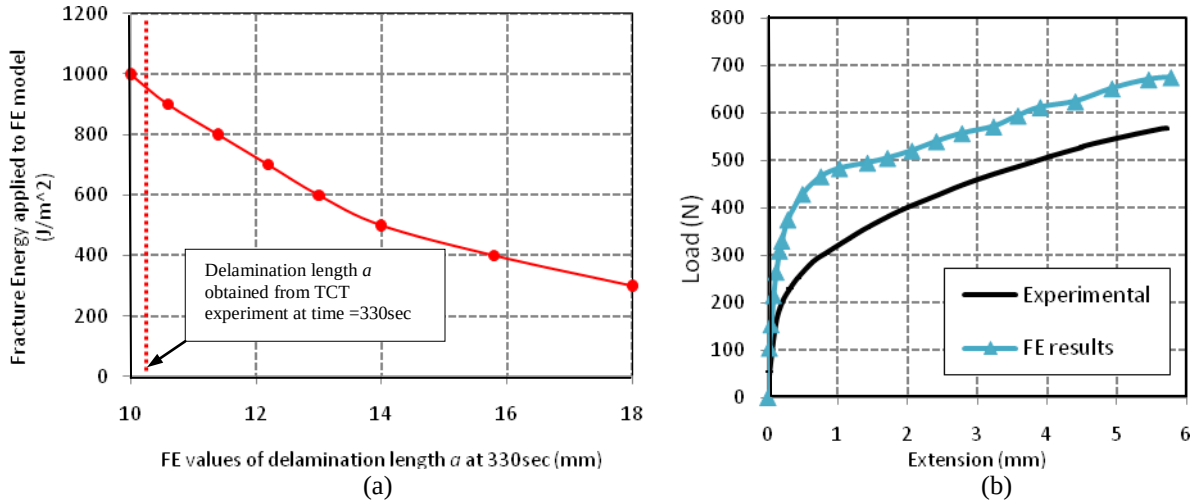

Figure 7: (a) Plot of Fracture Energy applied to FE model vs. delamination length (b) Plot of Load vs. extension curves from FE simulation and TCT experiment

8.0 ACKNOWLEDGEMENTS

We would like to thank Pilkington for providing us with laminated glass and samples of PVB.

9.0 REFERENCES

[1] Muralidhar, S., Jagota, A., Bennison, S. J. and Saigal, S. *Acta materialia*., 2000, 48, p4577-4588.

[2] Sha, Y., Hui, C. Y., Kramer, E. J., Garrett, P. D. and Knapczyk, J. W. J. *Adhesion Sci Tech.*, 1997, 11, 49.

[3] Iwasaki, R. and Sato, C. *J. Phys. IV* France. , 2006, 134, 1153-1158.

[4] Kinloch, A.J., Lau, C.C. and Williams, J.G., *Int. J. Fracture*, vol. 66, 45-70, 1994.

[5] BS EN ISO 527-1: 1996 and BS EN ISO 527-2: 1996 (BSI, 1996a)

[6] http://www.lusas.com/products/information/analysis_summary.html

[7] Overend, M., Jin, Q. and Watson, J. *Investigations into steel-glass adhesive joints.* SCI Innoglast Report, June 2010